HHS Public Access

Author manuscript

*Stroke*. Author manuscript; available in PMC 2017 November 28.

Published in final edited form as:

*Stroke*. 2015 December ; 46(12): 3514–3522. doi:10.1161/STROKEAHA.115.010767.

# Integrative mouse and human studies implicate *ANGPT1* and *ZBTB7C* as susceptibility genes to ischemic injury

**Rose Du, MD, PhD**[1,2,*], **Jing Zhou, PhD**[1], **Svetlana Lorenzano, MD, PhD**[3,4], **Wenming Liu, MD**[1,5], **Nareerat Charoenvimolphan, BA**[1], **Baogang Qian, MD**[1], **Jun Xu, MD**[1,6], **Jian Wang, MD, PhD**[1], **Xinmu Zhang, PhD**[1], **Xin Wang, PhD**[1], **Annerose Berndt, PhD**[7,8], **William J Devan, BA**[3,9], **Valerie J Valant, BA**[3,10], **Jinyi Wang, PhD**[5], **Karen L Furie, MD**[11], **Jonathan Rosand, MD**[3], **Natalia Rost, MD**[3], **Robert M Friedlander, MD**[12], **Beverly Paigen, PhD**[7], and **Scott T. Weiss, MD**[2]

[1]Department of Neurosurgery, Brigham and Women's Hospital, Boston, Massachusetts, USA

[2]Channing Division of Network Medicine, Brigham and Women's Hospital, Boston, Massachusetts, USA

[3]Department of Neurology, Massachusetts General Hospital, Boston, Massachusetts, USA

[4]Department of Neurology and Psychiatry, Sapienza University of Rome, Rome, Italy

[5]Department of Chemical Biology, Northwest Agriculture and Forestry University, Shaanxi, People's Republic of China

[6]Department of Neurosurgery, China-Japan Friendship Hospital, Beijing, People's Republic of China

[7]The Jackson Laboratory, Bar Harbor, Maine, USA

[8]Division of Pulmonary, Allergy, and Critical Care Medicine, University of Pittsburgh School of Medicine, Pittsburgh, Pennsylvania, USA

[9]Quinnipiac University Frank H. Netter, MD School of Medicine, Hamden, Connecticut, USA

[10]University of Massachusetts Medical School, Worcester, Massachusetts, USA

[11]Department of Neurology, Warren Alpert Medical School of Brown University, Providence, Rhode Island, USA

[12]Department of Neurosurgery, University of Pittsburgh School of Medicine, Pittsburgh, Pennsylvania, USA

## Abstract

**Background and Purpose—**The extent of ischemic injury in response to cerebral ischemia is known to be affected by native vasculature. However, the non-vascular and dynamic vascular responses and their genetic basis are not well-understood.

**Corresponding author:** Rose Du, MD, PhD, Department of Neurosurgery, Brigham and Women's Hospital, 75 Francis Street, Boston, MA 02115, Fax: 617-734-8342, Phone: 617-732-6600, rdu@partners.org.

**Disclosures**

Svetlana Lorenzano is an expert consultant for Boehringer Ingelheim.

**Methods—**We performed a genome-wide association study in 235 mice from 33 inbred strains using the middle cerebral artery occlusion model. Population structure and genetic relatedness were accounted for by using the efficient mixed-model association method. Human orthologs to the genes associated with the significant and suggestive SNPs from the mouse strain survey were examined in patients with M1 occlusions admitted with signs and symptoms of acute ischemic stroke.

**Results—**We identified four genome-wide significant and suggestive SNPs to be associated with infarct volume in mice (rs3694965, $p=2.17\times10^{-7}$; rs31924033, $p=5.61\times10^{-6}$; rs32249495, $p=2.08\times10^{-7}$; rs3677406, $p=9.56\times10^{-6}$). Rs32249495, which corresponds to angiopoietin-1 (*ANGPT1*), was also significant in the recessive model in humans, while rs1944577, which corresponds to *ZBTB7C* was nominally significant in both the additive and dominant genetic models in humans. *ZBTB7C* was shown to be upregulated in endothelial cells using both *in vitro* and *in vivo* models of ischemia.

**Conclusions—**Genetic variations of *ANGPT1* and *ZBTB7C* are associated with increased infarct size in both mice and humans. *ZBTB7C* may modulate the ischemic response via neuronal apoptosis as well as dynamic collateralization and, in addition to *ANGPT1*, may serve as potential novel targets for treatments of cerebral ischemia.

### Keywords

stroke; genetics; animal models; cerebral infarction; cerebral ischemia

## Introduction

Cerebral ischemia remains a major public health concern with more than 20 million strokes occurring annually worldwide[1], making it the third leading cause of death[2] and the leading cause of adult disability[1]. It is widely accepted that the extent of cerebral infarction after an ischemic insult is dependent upon the degree of vascular collateralization. The contribution of the native vasculature to infarct volume has been shown in rodent models where different strains of mice exhibit different degrees of cerebral infarction after occlusion of the middle cerebral artery[3]. Investigation in a few strains of mice showed that the completeness of the circle of Willis, particularly the presence of the P1 segment of the posterior cerebral artery, contributes to the degree of cerebral perfusion and infarct size after occlusion of the middle cerebral artery[4, 5]. It has also been shown that native pial collaterals contribute to infarct size[6]. However, there are other factors beyond native vasculature that modulate ischemic damage. One of the other components is the dynamic remodeling of the vasculature that occurs with ischemic injury[7]. More recently, it has been shown that differences in infarct volume in different mouse strains using the distal middle cerebral artery occlusion model is associated with genetic variation in integrin alpha L that is independent of the effects of collaterals[8, 9]. In this study, we utilized the proximal middle cerebral artery occlusion model in 235 mice from 33 inbred strains to examine the genetic basis of the ischemic response. We have demonstrated in the mice examined that large vessel anatomy is not significantly correlated with infarct size. By integrating the strain survey results with human data, we identified *ANGPT1* and *ZBTB7C* as susceptibility genes for ischemic injury.

## Methods

### Middle cerebral artery occlusion model

Thirty-three inbred strains of mice were obtained from the Jackson Laboratory (Table 1). The permanent middle cerebral artery occlusion (MCAO) model was performed on 5 to 25 mice for each strain (total 235 mice) in a random order. Eight- to 10-week-old male mice (14–45 g) were used for the MCAO model. The MCAO model was performed as described previously[10] and detailed in the supplement. The number of mice excluded for each strain due to unsuccessful surgery or death is shown in Supplemental Table I. Physiological parameters for each strain of mice are detailed in Supplemental Table II. All animal housing, care, and experiments were performed according to the guidelines and regulations of the Institutional Animal Care and Use Committee.

The brain was dissected into 1 mm coronal sections using a brain matrix and incubated in 2% triphenyltetrazolium chloride (TTC) (Sigma, St. Louis, MO) at room temperature for 15 minutes. The total infarct volume was calculated by summing the infarct area across all slices by an investigator blinded to the genetics data at the time of measurement. The indirect Swanson method[11] was used where the infarct ratio was defined as (contralateral volume − ipsilateral non-infarcted volume)/contralateral volume.

### Assessment of circle of Willis

The circle of Willis was visualized using India ink perfusion as described previously[12] and in the supplement. This was performed in 13 strains of mice: 129S1/SvImJ, A/J, BALB/cJ, BTBR $T^+$ tf/J, C57BL/10J, C57BL/6J, C57BLKS/J, C57L/J, DBA2/J, KK/HlJ, NOD/LtJ, P/J and SWR/J. 4–7 animals were used for each strain. The ratio of the diameter of the left P1 segment of the PCA to the diameter of the ICA at its bifurcation was measured using ImageJ 1.43 (NIH).

### Genome-wide association analysis

Genome-wide association mapping, with infarct ratio as the phenotype, was performed on the 33 inbred strains of mice using the R package, *emma*, where the efficient mixed-model association method was used to adjust for population structure and genetic relatedness in inbred mice[13]. The Broad mouse HapMap SNP sets containing 132,285 SNPs were used (http://www.broadinstitute.org/mouse/hapmap/, http://mouse.cs.ucla.edu/mousehapmap/emma.html). Using the R package *nortest*[14], the Anderson-Darling test of normality was used to evaluate normality of the infarct ratios. The p values were corrected for multiple testing by the Benjamini and Hochberg's false discovery rate algorithm (referred to as q value)[15]. SNPs with $p<10^{-5}$ were considered suggestive.

Associated genes were obtained within 500 kbp of each SNP from MGI Mart using the NCBIM37 dataset (http://biomart.informatics.jax.org). The rationale for this size window is to ensure that regulatory SNPs are included since most enhancers and repressors occur less than 500 kbp away from the gene[16]. Corresponding human orthologs of each gene was also obtained using MGI Mart. SNPs within each human gene were then obtained using the biomaRt package in R[17].

## Human middle cerebral artery occlusion

Consecutive Caucasian patients who were admitted to the Massachusetts General Hospital emergency department with signs and symptoms of acute ischemic stroke, who had only M1 occlusions, and who were genotyped were included in order to achieve a similar phenotype to the murine MCAO model. Thirty-three patients fit the inclusion criteria. Of those, 12 were female and 21 were male. 23 head CTs and 10 MRIs were performed on admission, prior to any thrombolytic therapy. The human portion of this study was approved by the Institutional Review Board.

CT and CT angiography (CTA), and/or MRI were performed on admission based on routine clinical stroke work-up and clinical requirements. For the purposes of this study, MRI diffusion-weighted imaging (DWI) performed at admission within 24 hours of symptom onset was used to assess the baseline infarct volume. All CT/CTAs used were performed at admission prior to thrombolytic treatment. Routine CTA imaging protocols for the diagnosis of large vessel occlusions adopted in the STOP-Stroke study was used and are reported elsewhere[18]. Patients who underwent at least a CT/CTA or MRI prior to thrombolytic therapy with an occlusion of the M1 division of the middle cerebral artery (MCA) were included. All lesion volumes were corrected for differences in overall brain size using mid-sagittal cross-sectional intracranial area as a surrogate measure of the intracranial volume[19]. All volumetric data were measured using a validated semi-automated protocol[20]. The intra-class correlation coefficient for the volumetric lesion analysis was 0.99 for DWI volume[21]. Imaging analyses were performed by an experienced and trained neurologist blinded to clinical and genetic data.

The Illumina Quad610 Beadchip and Affymetrix Human SNP Array 6.0 were used for genotyping. PLINK[22] was used to exclude SNPs that failed the Hardy-Weinberg equilibrium test ($p < 0.001$), had minor allele frequency < 1%, and had more than 5% of missing data. Additional SNPs were excluded using the linkage disequilibrium-based SNP pruning procedure in PLINK with a window size of 50, step of 5, and r^2 threshold of 0.5. The SNPs from the candidate genes were then extracted from the pruned set and analyzed.

A linear model was used to perform the association study using R with the normalized infarct volume as the phenotype and age, sex, genotyping platform, and imaging modality as covariates. The additive, dominant and recessive genetic models were evaluated. Adjustment for multiple testing was performed using the Benjamini and Hochberg correction[15].

## Oxygen glucose deprivation (OGD)

Ischemic conditions were modeled *in vitro* using the oxygen glucose deprivation model as previously described[23] on murine brain endothelial cell line (bEnd.3) derived from BALB/c mice and human umbilical vein endothelial cells (HUVECs) (see supplement). OGD is performed overnight (at least 16 hours). Cells were harvested immediately after termination of OGD. Three sets of experiments were performed for each cell type for a total of 6 control and 10 OGD cultures for murine endothelial cell lines and 6 control and 9 OGD cultures for HUVECs.

### Real-time PCR analysis

Quantitative real-time PCR was performed as described previously[24] and detailed in the supplement to determine expression of ZBTB7C. Relative gene expression was determined using the $2^{-\Delta\Delta C_T}$ method and assessed by the t-test.

### Immunohistochemistry

Immunohistochemistry was done as previously described[25] (see supplement for details). The following primary antibodies and dilutions were used: ZBTB7C (1:50, rabbit polyclonal, Abcam, Cambridge, MA); NeuN (1:200, mouse monoclonal, Abcam); GFAP (1:200, mouse monoclonal, Abcam); CD31 (1:100, rat monoclonal, BD Pharmingen, San Jose, CA). Fluorescent secondary antibodies, AlexaFluor488 or AlexaFluor594 (1:500 for ZBTB7C and 1:200 for all others, Molecular Probes, Eugene, OR), were used.

**Quantification of staining—**For quantification of ZBTB7C staining, we selected five random fields from the cortex on coronal sections of each of 3 MCAO and 3 control SWR/J mice. The ratio of ZBTB7C+NeuN+, ZBTB7C+CD31+, and ZBTB7C+GFAP+ cells to NeuN+, CD31+, and GFAP+ cells were obtained to determine the fraction of ZBTB7C+ neurons, endothelial cells, and astrocytes, respectively. Differences in the proportions of ZBTB7C+ cells in each cell type were assessed using the t-test.

### Statistical analysis

Statistical analysis was performed using the Wilcoxon signed rank test, Welch's t-test, and linear regression in R (version 3.0.2). P-values less than 0.05 were considered statistically significant. In the cases of genome-wide association testing, q-values less than 0.05 were considered genome-wide significant.

## Results

### Identification of candidate genes for susceptibility to ischemic injury in inbred mice

The infarct ratios for 33 inbred strains of mice measured 24 hours after middle cerebral artery occlusion (MCAO) are shown in Figure 1. The infarct ratios ranged from 0.40 to 0.78. The Anderson-Darling test of normality demonstrated that the infarct ratio is approximately normally distributed ($p=0.16$). There was no association between age, weight, or mean arterial pressure with infarct ratio ($p>0.05$).

**Completeness of the circle of Willis—**We examined the circle of Willis in 13 strains of mice with infarct ratios ranging from 0.40 to 0.78 to capture the full range of infarct ratios. In particular, we examined the ratio of left P1 diameter to left ICA diameter (Figure 1). The left P1 was chosen since we performed a left MCAO model but the results are similar for the right P1. Pearson's correlation between the infarct ratio and the left P1/ICA ratio was 0.049 ($p=0.88$). There was therefore no apparent correlation between infarct ratio and completeness of the circle of Willis in the strains examined. The proximal MCAO model could therefore be used without significant confounding by variations of the circle of Willis. This also avoids the problem of branch selection in a distal MCAO model.

**Genome-wide association testing—**Using the efficient mixed model association (EMMA) to account for population stratification among inbred strains of mice, we found two genome-wide significant SNPs (rs32249495, $p=2.02\times10^{-7}$; rs3694965, $p=2.05\times10^{-7}$) and two suggestive SNPs with $p < 10^{-5}$ (rs31924033, $p=5.50\times10^{-6}$; rs3677406, $p=9.31\times10^{-6}$) (Figure 1, Table 2).

## Association of *ZBTB7C* polymorphisms in human dataset

There were 38 genes within 500 kbp of the 4 significant and suggestive mouse SNPs (Figure 2). These genes were associated with 24 human orthologs. The 24 human genes contain 36,179 SNPs, 99 of which were common among the included ischemic stroke datasets. Among 33 Caucasian subjects with M1 occlusions, the acute infarct volumes ranged from 1.2 to 249.2 $cm^3$ (Figure 2). The 99 SNPs common to the ischemic stroke datasets that correspond to the 24 human orthologs were examined for association with infarct volume in patients with M1 occlusions (Figure 2, Table 3). The additive genetic model yielded 4 nominally significant SNPs (rs1944577, p=0.011; rs2514830, p=0.015; rs8043555, p=0.020; rs11074858, p=0.046) corresponding to the genes *ZBTB7C, RSPO2, KIAA0556*, and *IL21R*, respectively. The dominant model yielded 5 nominally significant SNPs (rs1944577, p=0.006; rs8043555, p=0.020; rs11639671, p=0.040; rs11074858, p=0.042; rs1489169, p=0.046) corresponding to the genes *ZBTB7C, KIAA0556, GSG1L, IL21R*, and *ZBTB7C*, respectively. The recessive model yielded 7 nominally significant SNPs (rs1283687, $p=3.94\times10^{-4}$; rs10163610, p=0.008; rs2514830, p=0.021; rs3091235, p=0.026; rs2189521, p=0.032; rs12934152, p=0.036; rs1000031, p=0.046) corresponding to the genes *ANGPT1, ZBTB7C, RSPO2, IL21R, IL21R, IL21R*, and *CTIF*, respectively. *ANGPT1* (angiopoietin-1) remained significant in the recessive model after adjustment for multiple testing (q=0.039), while the others did not.

## *ZBTB7C* expression is increased in endothelial cells after ischemia

As *ANGPT1* has been well-studied in the context of cerebral ischemia, we proceeded to further characterize *ZBTB7C*. Analysis of Gene Expression Omnibus datasets GSE26500 and GSE26844 did not demonstrate a difference in baseline expression of *ZBTB7C* (see supplement) across strains. This suggests that the difference in expression of *ZBTB7C* may occur in the ischemic or hypoxic setting rather than at baseline. We thus investigated the expression of *ZBTB7C* under ischemic/hypoxic conditions using the *in vivo* MCAO model and the *in vitro* oxygen glucose deprivation model (OGD). *ZBTB7C* expression in the MCAO model was performed using SWR/J and DBA2/J mice where SWR/J had a high infarct ratio of 0.77 while DBA2/J had a low infarct ratio of 0.50.

Quantitative PCR was performed on whole brain extracts to determine the expression of *ZBTB7C* 24 hours after MCAO compared to control mice (Figure 3). For DBA2/J mice, there was no difference in *ZBTB7C* expression between the MCAO hemisphere and control (p=0.170) while there was a significant difference in SWR/J mice (p=0.016). There was also a significant difference in *ZBTB7C* expression between the MCAO hemispheres of SWR/J and DBA2/J mice (p=0.010). This demonstrates that the most marked difference in ZBTB7C expression occurs after ischemic or hypoxic injury rather than at baseline.

To determine the cell types in which *ZBTB7C* expression occurs, we performed immunohistochemical analysis on control and MCAO mice of the SWR/J strain (Figure 3). We found that there is a significant increase in *ZBTB7C* expression in CD31+ endothelial cells in the MCAO hemisphere compared to the contralateral hemisphere and control ($p=1.89\times10^{-4}$ and $8.46\times10^{-6}$, respectively). There was no significant difference in *ZBTB7C* expression in astrocytic (GFAP+) or neuronal (NeuN+) cells.

To confirm this finding in the *in vitro* model, we performed oxygen glucose deprivation experiments on HUVECs and murine endothelial cell lines. The *in vitro* results are consistent with the above immunohistochemical analysis. *ZBTB7C* expression was assessed by quantitative real-time PCR (Figure 3). There was a significant increase in relative *ZBTB7C* expression by real-time PCR in HUVECs and endothelial cells under OGD compared to controls (relative expression 2.90 and 1.62, p=0.031 and 0.006, respectively).

## Discussion

While many genetic studies have been performed on risk of ischemic stroke[26–29], few have focused on the susceptibility to ischemic damage[8, 9]. The two questions are fundamentally different as the former addresses the propensity to develop stroke due to factors such as atherosclerotic disease, while the latter addresses the likelihood of ischemic damage given the presence of an ischemic insult. Understanding the basis of this susceptibility to ischemic damage can lead to the development of new therapeutic strategies.

To understand the genetic basis for such susceptibility, we integrated the results from a mouse model with human data. Strain differences in infarct size in the presence of focal ischemia has been shown in a few strains to be related to the completeness of the circle of Willis, particularly that of the P1 segment of the posterior cerebral artery (frequently denoted as posterior communicating artery in rodents)[4, 5]. We have demonstrated that across the strains examined in this study, the infarct size is independent of the circle of Willis. As such, the proximal MCAO model could be used. Such a model obviates the need for a craniotomy for intracranial exposure of the vasculature or for selection of a distal branch as is done in distal occlusion models, which may potentially have effects on the ischemic response.

Infarct volume has been shown to be associated with native pial collateral circulation[6]. The extent of such collateral circulation has been shown to have a genetic association[6, 30]. In particular, Wang et al. have demonstrated two QTLs on chromosome 7 to be associated with collateral numbers[30]. In addition, however, after ischemia, a number of vascular changes occur such as increases in vascular density, branching and collateral development[7] that are independent of the native collateral numbers. These changes will also affect the degree of ischemic damage. Moreover, it has been shown that there is a genetic effect on ischemic tolerance beyond the effects of the vasculature. Keum et al. have shown that genetic variation in *Itgal* modulates ischemic brain injury beyond vascular effects[8].

In our study, we identified *ZBTB7C* and *ANGPT1* as candidate genes for the association with susceptibility to ischemic injury. While animal models of ischemia are attractive

because of the ability to control environmental and ischemic conditions, the relevance of the findings to humans remains an important consideration. A SNP associated with *ZBTB7C* was identified as the most significant SNP in a human cohort in both the additive and dominant genetic models, while *ANGPT1* was associated with the most significant SNP in the human recessive model. The convergence of the findings across both mouse models and humans further strengthens the evidence for *ANGPT1* and *ZBTB7C* as potential significant mediators of ischemic injury.

ZBTB7C is a protein that contains an N-terminal BTB/POZ domain that is known to mediate protein–protein interaction and four DNA-binding $C_2H_2$ zinc finger domains[31]. It is highly expressed in the brain[32]. Our data for baseline expression of ZBTB7C is consistent with previous work by Zhang et al. with the expression by neurons and astrocytes approximately 7 to 9 fold higher than that of brain endothelial cells (http://web.stanford.edu/group/barres_lab/brain_rnaseq.html)[33]. We did not find differential expression of ZBTB7C at baseline among the mouse strains that correlated with infarct size, suggesting that ZBTB7C is unlikely to be involved in the formation of native collaterals. On the other hand, ZBTB7C is significantly upregulated in endothelial cells under ischemic conditions. While such an association does not prove causality, prior studies have shown that ZBTB7C is involved in pathways that would result in increased neuronal death[34–36], decreased formation of vascular network[37], and endothelial dysfunction[36].

ZBTB7C has been described as participating in two different pathways, via its interaction with p53 and SREBP1c (Supplemental Figure I). ZBTB7C has been shown to physically interact with and inhibit p53, a transcriptional activator of p21[38], thereby negatively regulating p21. P21 has been shown to be antiapoptotic in neurons[34] via cell-cycle dependent[39] and independent pathways[40]. Under mild oxidative stress, p21 upregulates Nrf2 which is a transcription factor that activates an antioxidant response that protects against cellular damage[41] including that of ischemic neurons[35], and also stimulates the formation of vascular networks[37]. On the other hand, under moderate oxidative stress p21 initiates cell cycle arrest to allow DNA repair in response to DNA damage[41]. ZBTB7C thus increases apoptosis in neurons and inhibits the formation of vascular network via the p53/p21 pathway, both of which would lead to increased ischemic damage.

As an alternative pathway, ZBTB7C has also been shown to interact with and enhance the activity of sterol regulatory element binding protein-1c (SREBP-1c)[42]. SREBP-1 has been shown to increase neuronal damage during ischemia[36]. In addition, SREBP1c has been shown to be a repressor of dimethylarginine dimethyl-aminohydrolase (DDAH1) with resultant increase in asymmetric dimethylarginine (ADMA), decrease in nitric oxide synthase, and resulting endothelial dysfunction[36]. An increase in ZBTB7C may thus increase ischemic neuronal damage and increase endothelial dysfunction via the SREBP-1c pathway.

The involvement of ZBTB7C in the formation of vascular networks suggests that it may play a role in the dynamic collateralization process after ischemia, in addition to modulating neuronal apoptosis. The specific mechanism by which this occurs would require further study.

Beside *ZBTB7C, ANGPT1* was also associated with the response to ischemia in both mice and humans and was significant after adjustment for multiple testing in both. *ANGPT1* is expressed in astrocytes, neurons, pericytes and endothelial cells but is predominantly expressed by astrocytes in the brain[43–46]. Angiopoietin-1 has previously been shown to reduce infarct size by stabilizing endothelial cell integrity, reducing blood brain barrier permeability, and promoting angiogenesis[47–49]. It has also been shown to be a regulator of microvascular tone[50]. *ANGPT1* therefore, like *ZBTB7C*, modulates ischemic injury independently of native collaterals, but does so via astrocytes that are in close contact with the endothelial cells.

### Limitations

Our findings should be considered in the context of some important limitations. First, although we demonstrated that there is no significant correlation between the completeness of the circle of Willis via the P1 segment and the infarct size in the mouse strains examined, such an effect may still confound the results. A number of mice were excluded due to unsuccessful surgery or death. This may lead to attrition bias. Since the researcher was not blinded to the strain of mice undergoing surgery, this may introduce additional bias. Furthermore, while the *ZBTB7C* and *ANGPT1* baseline expressions were not associated with infarct size, the genetic variations may still be associated with the native collateral formation via mechanisms other than gene expression. In addition, the human dataset used was small. Further replication of our results in a larger human cohort is warranted. Finally, while it is plausible from prior work that the increase in ZBTB7C is involved in dynamic collateralization and neuronal apoptosis, further studies utilizing ZBTB7C knockout mice and knockdown/overexpressing endothelial cells to examine the specific mechanism is still required.

## Conclusions

While it is known that the extent of cerebral infarction is dependent on native collaterals, there is increasing evidence that there are also dynamic vascular and non-vascular modulators of ischemic damage. By integrating mouse and human data, we demonstrated an association between genetic variations of *ANGPT1* and *ZBTB7C* and the extent of ischemic damage. *ZBTB7C* may act via modulation of neuronal apoptosis, as well as dynamic collateralization and endothelial dysfunction while *ANGPT1* has been shown to affect endothelial integrity and angiogenesis. Together, *ZBTB7C* and *ANGPT1* may provide potential targets for novel treatments of cerebral ischemia.

## Supplementary Material

Refer to Web version on PubMed Central for supplementary material.

## Acknowledgments

**Funding Sources**

This work was supported by the National Institutes of Health grant K08NS067172 and by the Anspach Research Award (to R.D.).

## References


1. Bakhai A. The burden of coronary, cerebrovascular and peripheral arterial disease. Pharmacoeconomics. 2004; 22(Suppl 4):11–18. [PubMed: 15876008]
2. Johnston SC. The 2008 william m. Feinberg lecture: Prioritizing stroke research. Stroke. 2008; 39:3431–3436. [PubMed: 18818399]
3. Yang G, Kitagawa K, Matsushita K, Mabuchi T, Yagita Y, Yanagihara T, et al. C57bl/6 strain is most susceptible to cerebral ischemia following bilateral common carotid occlusion among seven mouse strains: Selective neuronal death in the murine transient forebrain ischemia. Brain research. 1997; 752:209–218. [PubMed: 9106459]
4. Fujii M, Hara H, Meng W, Vonsattel JP, Huang Z, Moskowitz MA. Strain-related differences in susceptibility to transient forebrain ischemia in sv-129 and c57black/6 mice. Stroke; a journal of cerebral circulation. 1997; 28:1805–1810. discussion 1811.
5. Kitagawa K, Matsumoto M, Yang G, Mabuchi T, Yagita Y, Hori M, et al. Cerebral ischemia after bilateral carotid artery occlusion and intraluminal suture occlusion in mice: Evaluation of the patency of the posterior communicating artery. Journal of cerebral blood flow and metabolism : official journal of the International Society of Cerebral Blood Flow and Metabolism. 1998; 18:570–579.
6. Zhang H, Prabhakar P, Sealock R, Faber JE. Wide genetic variation in the native pial collateral circulation is a major determinant of variation in severity of stroke. Journal of cerebral blood flow and metabolism : official journal of the International Society of Cerebral Blood Flow and Metabolism. 2010; 30:923–934.
7. Bailey AM, O'Neill TJt, Morris CE, Peirce SM. Arteriolar remodeling following ischemic injury extends from capillary to large arteriole in the microcirculation. Microcirculation. 2008; 15:389–404. [PubMed: 18574742]
8. Keum S, Lee HK, Chu PL, Kan MJ, Huang MN, Gallione CJ, et al. Natural genetic variation of integrin alpha l (itgal) modulates ischemic brain injury in stroke. PLoS genetics. 2013; 9:e1003807. [PubMed: 24130503]
9. Keum S, Marchuk DA. A locus mapping to mouse chromosome 7 determines infarct volume in a mouse model of ischemic stroke. Circulation. Cardiovascular genetics. 2009; 2:591–598. [PubMed: 20031639]
10. Friedlander RM, Gagliardini V, Hara H, Fink KB, Li W, MacDonald G, et al. Expression of a dominant negative mutant of interleukin-1 beta converting enzyme in transgenic mice prevents neuronal cell death induced by trophic factor withdrawal and ischemic brain injury. The Journal of experimental medicine. 1997; 185:933–940. [PubMed: 9120399]
11. Swanson RA, Sharp FR. Infarct measurement methodology. Journal of cerebral blood flow and metabolism : official journal of the International Society of Cerebral Blood Flow and Metabolism. 1994; 14:697–698.
12. McGirt MJ, Lynch JR, Parra A, Sheng H, Pearlstein RD, Laskowitz DT, et al. Simvastatin increases endothelial nitric oxide synthase and ameliorates cerebral vasospasm resulting from subarachnoid hemorrhage. Stroke; a journal of cerebral circulation. 2002; 33:2950–2956.
13. Kang HM, Zaitlen NA, Wade CM, Kirby A, Heckerman D, Daly MJ, et al. Efficient control of population structure in model organism association mapping. Genetics. 2008; 178:1709–1723. [PubMed: 18385116]
14. Gross J, Ligges U. Nortest: Tests for normality. R package version 1.0-4. 2015
15. Benjamini Y, Hochberg Y. Controlling the false discovery rate: A practical and powerful approach to multiple testing. J R Statist Soc B. 1995; 57:289–300.
16. Wang K, Li M, Bucan M. Pathway-based approaches for analysis of genomewide association studies. American journal of human genetics. 2007; 81:1278–1283. [PubMed: 17966091]
17. Durinck S, Spellman PT, Birney E, Huber W. Mapping identifiers for the integration of genomic datasets with the r/bioconductor package biomart. Nature protocols. 2009; 4:1184–1191. [PubMed: 19617889]

18. Smith WS, Lev MH, English JD, Camargo EC, Chou M, Johnston SC, et al. Significance of large vessel intracranial occlusion causing acute ischemic stroke and tia. Stroke; a journal of cerebral circulation. 2009; 40:3834–3840.
19. Ferguson KJ, Wardlaw JM, Edmond CL, Deary IJ, Maclullich AM. Intracranial area: A validated method for estimating intracranial volume. Journal of neuroimaging : official journal of the American Society of Neuroimaging. 2005; 15:76–78. [PubMed: 15574578]
20. Gurol ME, Irizarry MC, Smith EE, Raju S, Diaz-Arrastia R, Bottiglieri T, et al. Plasma beta-amyloid and white matter lesions in ad, mci, and cerebral amyloid angiopathy. Neurology. 2006; 66:23–29. [PubMed: 16401840]
21. Ay H, Arsava EM, Vangel M, Oner B, Zhu M, Wu O, et al. Interexaminer difference in infarct volume measurements on mri: A source of variance in stroke research. Stroke; a journal of cerebral circulation. 2008; 39:1171–1176.
22. Purcell S, Neale B, Todd-Brown K, Thomas L, Ferreira MA, Bender D, et al. Plink: A tool set for whole-genome association and population-based linkage analyses. American journal of human genetics. 2007; 81:559–575. [PubMed: 17701901]
23. Wang X, Figueroa BE, Stavrovskaya IG, Zhang Y, Sirianni AC, Zhu S, et al. Methazolamide and melatonin inhibit mitochondrial cytochrome c release and are neuroprotective in experimental models of ischemic injury. Stroke; a journal of cerebral circulation. 2009; 40:1877–1885.
24. Du R, Lu KV, Petritsch C, Liu P, Ganss R, Passegue E, et al. Hif1alpha induces the recruitment of bone marrow-derived vascular modulatory cells to regulate tumor angiogenesis and invasion. Cancer cell. 2008; 13:206–220. [PubMed: 18328425]
25. Du R, Petritsch C, Lu K, Liu P, Haller A, Ganss R, et al. Matrix metalloproteinase-2 regulates vascular patterning and growth affecting tumor cell survival and invasion in gbm. Neuro-oncology. 2008; 10:254–264. [PubMed: 18359864]
26. Kilarski LL, Achterberg S, Devan WJ, Traylor M, Malik R, Lindgren A, et al. Meta-analysis in more than 17,900 cases of ischemic stroke reveals a novel association at 12q24.12. Neurology. 2014; 83:678–685. [PubMed: 25031287]
27. Cotlarciuc I, Malik R, Holliday EG, Ahmadi KR, Pare G, Psaty BM, et al. Effect of genetic variants associated with plasma homocysteine levels on stroke risk. Stroke; a journal of cerebral circulation. 2014; 45:1920–1924.
28. Williams SR, Yang Q, Chen F, Liu X, Keene KL, Jacques P, et al. Genome-wide meta-analysis of homocysteine and methionine metabolism identifies five one carbon metabolism loci and a novel association of aldh1l1 with ischemic stroke. PLoS genetics. 2014; 10:e1004214. [PubMed: 24651765]
29. Traylor M, Farrall M, Holliday EG, Sudlow C, Hopewell JC, Cheng YC, et al. Genetic risk factors for ischaemic stroke and its subtypes (the metastroke collaboration): A meta-analysis of genome-wide association studies. The Lancet. Neurology. 2012; 11:951–962. [PubMed: 23041239]
30. Wang S, Zhang H, Dai X, Sealock R, Faber JE. Genetic architecture underlying variation in extent and remodeling of the collateral circulation. Circulation research. 2010; 107:558–568. [PubMed: 20576932]
31. Reuter S, Bartelmann M, Vogt M, Geisen C, Napierski I, Kahn T, et al. Apm-1, a novel human gene, identified by aberrant co-transcription with papillomavirus oncogenes in a cervical carcinoma cell line, encodes a btb/poz-zinc finger protein with growth inhibitory activity. The EMBO journal. 1998; 17:215–222. [PubMed: 9427755]
32. Gilling M, Lind-Thomsen A, Mang Y, Bak M, Moller M, Ullmann R, et al. Biparental inheritance of chromosomal abnormalities in male twins with non-syndromic mental retardation. European journal of medical genetics. 2011; 54:e383–388. [PubMed: 21426945]
33. Zhang Y, Chen K, Sloan SA, Bennett ML, Scholze AR, O'Keeffe S, et al. An rna-sequencing transcriptome and splicing database of glia, neurons, and vascular cells of the cerebral cortex. The Journal of neuroscience : the official journal of the Society for Neuroscience. 2014; 34:11929–11947. [PubMed: 25186741]
34. Harms C, Albrecht K, Harms U, Seidel K, Hauck L, Baldinger T, et al. Phosphatidylinositol 3-akt-kinase-dependent phosphorylation of p21(waf1/cip1) as a novel mechanism of neuroprotection by

glucocorticoids. The Journal of neuroscience : the official journal of the Society for Neuroscience. 2007; 27:4562–4571. [PubMed: 17460069]

35. Shah ZA, Li RC, Ahmad AS, Kensler TW, Yamamoto M, Biswal S, et al. The flavanol (−)-epicatechin prevents stroke damage through the nrf2/ho1 pathway. Journal of cerebral blood flow and metabolism : official journal of the International Society of Cerebral Blood Flow and Metabolism. 2010; 30:1951–1961.
36. Ivashchenko CY, Bradley BT, Ao Z, Leiper J, Vallance P, Johns DG. Regulation of the adma-ddah system in endothelial cells: A novel mechanism for the sterol response element binding proteins, srebp1c and -2. American journal of physiology. Heart and circulatory physiology. 2010; 298:H251–258. [PubMed: 19915177]
37. Florczyk U, Jazwa A, Maleszewska M, Mendel M, Szade K, Kozakowska M, et al. Nrf2 regulates angiogenesis: Effect on endothelial cells, bone marrow-derived proangiogenic cells and hind limb ischemia. Antioxidants & redox signaling. 2014; 20:1693–1708. [PubMed: 24053644]
38. Jeon BN, Kim MK, Choi WI, Koh DI, Hong SY, Kim KS, et al. Kr-pok interacts with p53 and represses its ability to activate transcription of p21waf1/cdkn1a. Cancer research. 2012; 72:1137–1148. [PubMed: 22253232]
39. Mallick S, D'Mello SR. Jaz (znf346), a sirt1-interacting protein protects neurons by stimulating p21 (waf/cip1) expression. The Journal of biological chemistry. 2014
40. Langley B, D'Annibale MA, Suh K, Ayoub I, Tolhurst A, Bastan B, et al. Pulse inhibition of histone deacetylases induces complete resistance to oxidative death in cortical neurons without toxicity and reveals a role for cytoplasmic p21(waf1/cip1) in cell cycle-independent neuroprotection. The Journal of neuroscience : the official journal of the Society for Neuroscience. 2008; 28:163–176. [PubMed: 18171934]
41. Villeneuve NF, Sun Z, Chen W, Zhang DD. Nrf2 and p21 regulate the fine balance between life and death by controlling ros levels. Cell cycle. 2009; 8:3255–3256. [PubMed: 19806015]
42. Jeon BN, Kim YS, Choi WI, Koh DI, Kim MK, Yoon JH, et al. Kr-pok increases fasn expression by modulating the DNA binding of srebp-1c and sp1 at the proximal promoter. Journal of lipid research. 2012; 53:755–766. [PubMed: 22331133]
43. Horton BN, Solanki RB, Rajneesh KF, Kulesza P, Ardelt AA. Localization of angiopoietin-1 and tie2 immunoreactivity in rodent ependyma and adjacent blood vessels suggests functional relationships. The journal of histochemistry and cytochemistry : official journal of the Histochemistry Society. 2010; 58:53–60. [PubMed: 19786610]
44. Hori S, Ohtsuki S, Hosoya K, Nakashima E, Terasaki T. A pericyte-derived angiopoietin-1 multimeric complex induces occludin gene expression in brain capillary endothelial cells through tie-2 activation in vitro. Journal of neurochemistry. 2004; 89:503–513. [PubMed: 15056293]
45. Zacharek A, Chen J, Cui X, Li A, Li Y, Roberts C, et al. Angiopoietin1/tie2 and vegf/flk1 induced by msc treatment amplifies angiogenesis and vascular stabilization after stroke. Journal of cerebral blood flow and metabolism : official journal of the International Society of Cerebral Blood Flow and Metabolism. 2007; 27:1684–1691.
46. Koyama Y, Maebara Y, Hayashi M, Nagae R, Tokuyama S, Michinaga S. Endothelins reciprocally regulate vegf-a and angiopoietin-1 production in cultured rat astrocytes: Implications on astrocytic proliferation. Glia. 2012; 60:1954–1963. [PubMed: 22927341]
47. Meng Z, Li M, He Q, Jiang S, Zhang X, Xiao J, et al. Ectopic expression of human angiopoietin-1 promotes functional recovery and neurogenesis after focal cerebral ischemia. Neuroscience. 2014; 267:135–146. [PubMed: 24607344]
48. Valable S, Montaner J, Bellail A, Berezowski V, Brillault J, Cecchelli R, et al. Vegf-induced bbb permeability is associated with an mmp-9 activity increase in cerebral ischemia: Both effects decreased by ang-1. Journal of cerebral blood flow and metabolism : official journal of the International Society of Cerebral Blood Flow and Metabolism. 2005; 25:1491–1504.
49. Zhang ZG, Zhang L, Croll SD, Chopp M. Angiopoietin-1 reduces cerebral blood vessel leakage and ischemic lesion volume after focal cerebral embolic ischemia in mice. Neuroscience. 2002; 113:683–687. [PubMed: 12150788]
50. Alfieri A, Ong AC, Kammerer RA, Solanky T, Bate S, Tasab M, et al. Angiopoietin-1 regulates microvascular reactivity and protects the microcirculation during acute endothelial dysfunction:

Role of enos and ve-cadherin. Pharmacological research : the official journal of the Italian Pharmacological Society. 2014; 80:43–51.

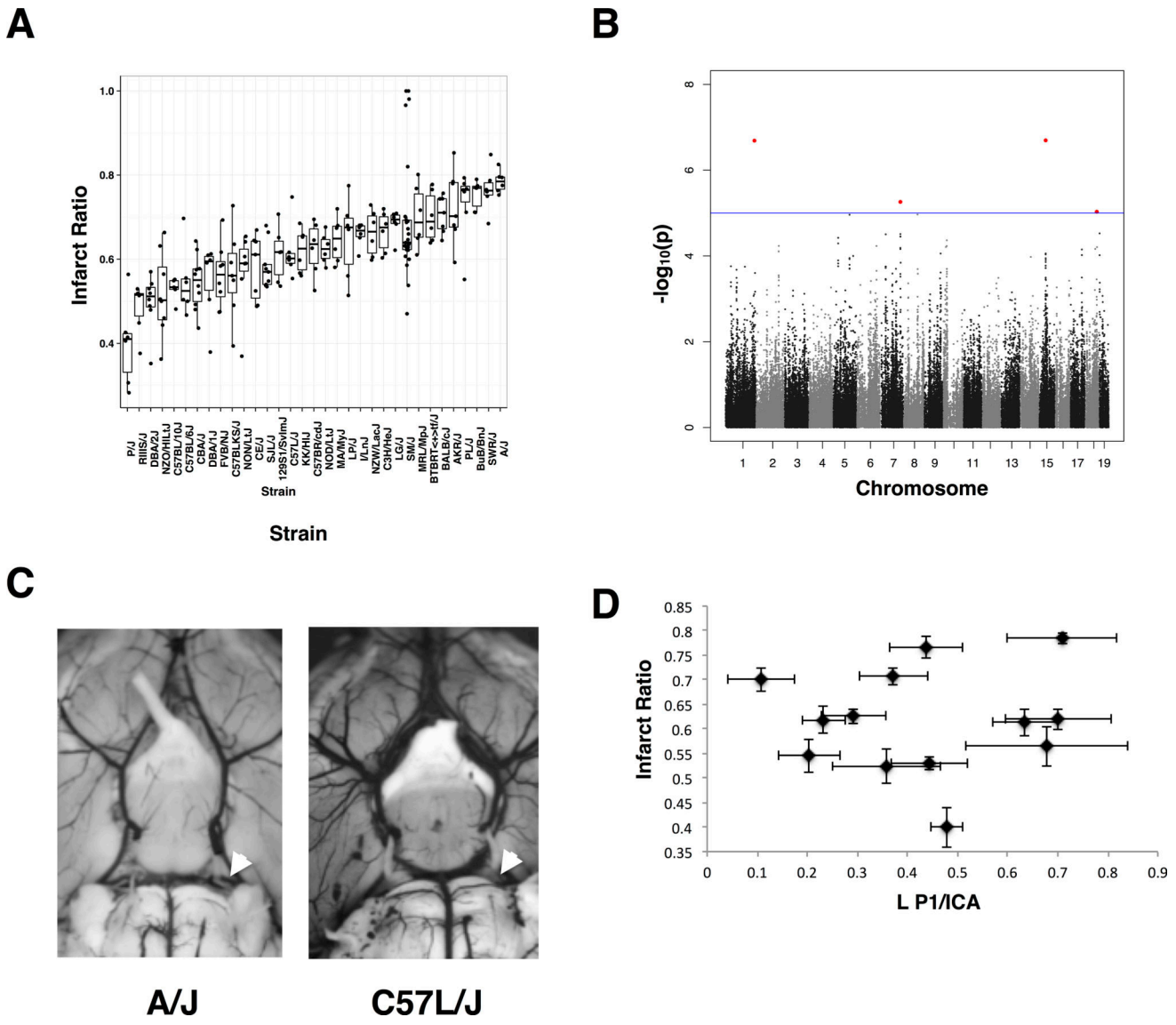


**Figure 1. Genome-wide association analysis using mouse stroke model**

A) Infarct ratios of 33 strains of inbred mice measured 24 hours after occlusion of the left middle cerebral artery. Infarct ratio was calculated using the Swanson method. B) Genome-wide association analysis of infarct ratio in the middle cerebral artery occlusion model with genome-wide p-values using the efficient mixed model association (EMMA). Blue line is the suggestive significance line set at $p = 10^{-5}$. C) Circle of Willis in A/J mouse and C57L/J mouse demonstrating large and small P1s, respectively. The vasculature is visualized with India ink perfusion. D) Correlation between infarct ratio and the completeness of the circle of Willis assessed with the ratio of the left P1 to left ICA diameters. Error bars are standard errors.

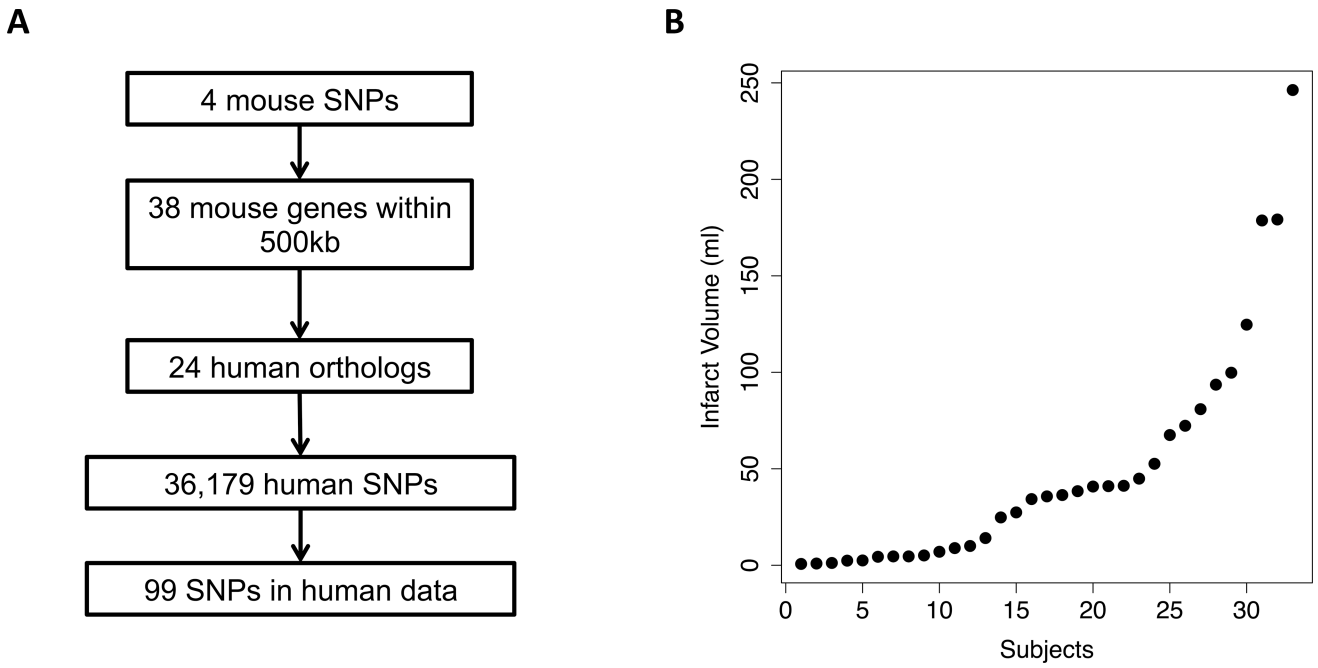


**Figure 2. Infarct volume in human middle cerebral artery occlusion**

A) Algorithm for obtaining human SNPs given mouse data. B) Infarct volume ($cm^3$) from 33 Caucasian patients with M1 occlusions.

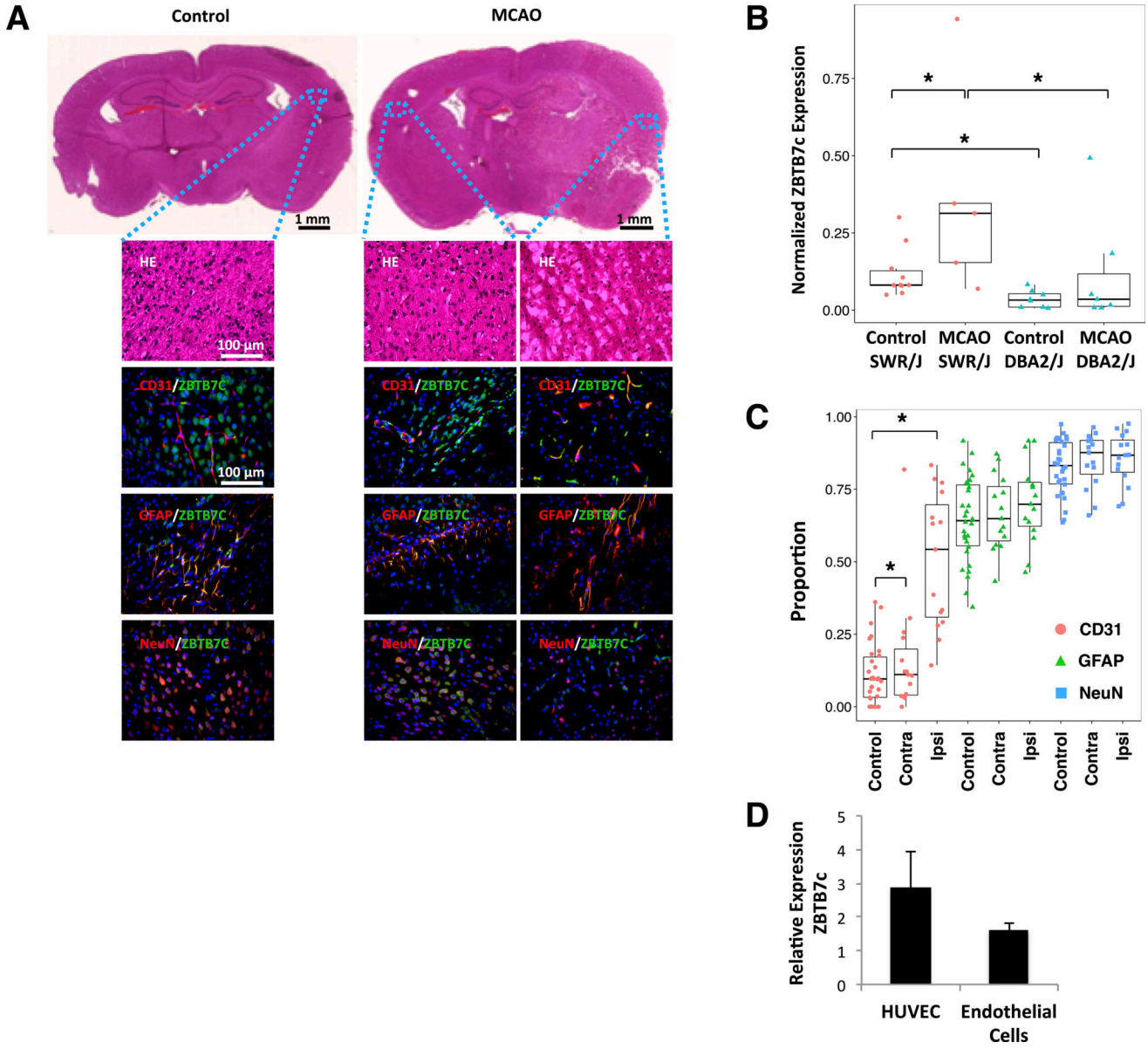


**Figure 3. *ZBTB7C* expression**

A) Representative immunohistochemical staining of normal and infarcted cortical regions for ZBTB7C (green), endothelial cell marker CD31 (red), astrocytic marker GFAP (red), and neuronal marker NeuN (red) in SWR/J control and MCAO mice. Scale bar is 100 μm. B) Strain-specific difference in expression of *ZBTB7C* after middle cerebral artery occlusion compared to control mice using quantitative PCR. C) Comparison of proportions of CD31+, GFAP+, and NeuN+ cells that also express ZBTB7C in SWR/J mice after MCAO in the ipsilateral hemisphere, contralateral hemisphere and in control mice. D) Quantitative PCR analysis showing relative expression of *ZBTB7C* in HUVECs (6 control, 9 OGD) and murine endothelial cell line (6 control, 10 OGD) under oxygen glucose deprivation compared to controls. There was a significant increase in expression in both HUVECs and murine endothelial cells. * indicates $p<0.05$. Error bars are standard errors.

**Table 1**

Inbred mouse strains.

| Strain | N |
|---|---|
| 129S1/SvImJ | 6 |
| A/J | 6 |
| AKR/J | 7 |
| BALB/cJ | 7 |
| BTBR $T^{+}$ tf/J | 6 |
| BUB/BnJ | 6 |
| C3H/HeJ | 6 |
| C57BL/10J | 5 |
| C57BL/6J | 6 |
| C57BLKS/J | 7 |
| C57BR/cdJ | 6 |
| C57L/J | 6 |
| CBA/J | 10 |
| CE/J | 7 |
| DBA/1J | 6 |
| DBA/2J | 8 |
| FVB/NJ | 8 |
| I/LnJ | 6 |
| KK/HlJ | 6 |
| LG/J | 6 |
| LP/J | 6 |
| MA/MyJ | 6 |
| MRL/MpJ | 6 |
| NOD/LtJ | 6 |
| NON/LtJ | 7 |
| NZO/HlLtJ | 8 |
| NZW/LacJ | 6 |
| P/J | 6 |
| PL/J | 7 |
| RIIIS/J | 6 |
| SJL/J | 9 |
| SM/J | 25 |
| SWR/J | 6 |

**Table 2**

Genome-wide significant and suggestive SNPs from strain survey.

| SNP | Chr | Base Pair | Major /minor allele | MAF* | Mouse genes within 500 kbp (distance from SNP in kb) | Human orthologs | Beta† | P value | Q value ‡ |
|---|---|---|---|---|---|---|---|---|---|
| rs32249495 | 15 | 42869550 | C/T | 0.47 | *Angpt1 (361), Rspo2 (0), Eif3e (212), AC099621.2 (390), AC099621.1 (393), Ttc35 (439)* | *ANGPT1, RSPO2, EIF3E, EMC2* | −0.127 | $2.02 \times 10^{-7}$ | 0.014 |
| rs3694965 | 1 | 187607712 | T/C | 0.40 | *Mir194-1 (470), Mir215 (470), Rab3gap2 (500), Iars2 (454), Bpnt1 (426), Eprs (355), 9630028B13Rik (342), Slc30a10 (315), AC122845.1 (95), Lyplal1 (304), AC131980.1 (328)* | *RAB3GAP2, IARS2, BPNT1, EPRS, SLC30A10, NSA2, LYPLAL1* | −0.140 | $2.05 \times 10^{-7}$ | 0.014 |
| rs31924033 | 7 | 132528422 | C/A | 0.33 | *AC125160.1 (165), 4930533L02Rik (67), 4933440M02Rik (35), Jmjd5 (60), Nsmce1 (83), Il4ra (167), Il21r (219), Gtf3c1 (256), D430042O09Rik (323), AC150648.1 (496)* | *JMJD5, NSMCE1, IL4R, IL21R, GTF3C1, KIAA0556, GSG1L* | 0.128 | $5.50 \times 10^{-6}$ | 0.241 |
| rs3677406 | 18 | 75599810 | C/T | 0.23 | *Snord58b-201 (439), SNORD58.1-201 (439), SNORD58.2-201 (438), AC120176.1 (74), Zbtb7c (380), Lipg (479), Rpl17 (437), BC031181 (430), Dym (153), Smad7 (44), Gm672 (0)* | *ZBTB7C, LIPG, C18orf32, DYM, SMAD7, CTIF* | −0.149 | $9.31 \times 10^{-6}$ | 0.241 |

*MAF is minor allele frequency, based on the 33 strains of mice examined.

†Beta is the correlation coefficient between SNP and infarct ratio based on the minor allele from an additive model.

‡Q values were obtained using the Benjamini and Hochberg false discovery rate algorithm.

**Table 3**

Significant SNPs from human cohort.

| SNP | Chr | Base Pair | Major /minor allele | MAF * | Gene | Beta† | Raw p |
|---|---|---|---|---|---|---|---|
| **Additive Model** | | | | | | | |
| rs1944577 | 18 | 45730103 | C/T | 0.29 | ZBTB7C | −39.6 | 0.011 |
| rs2514830 | 8 | 109015548 | C/A | 0.39 | RSPO2 | 31.9 | 0.015 |
| rs8043555 | 16 | 27777831 | G/A | 0.14 | KIAA0556 | 49.1 | 0.020 |
| rs11074858 | 16 | 27429237 | C/T | 0.23 | IL21R | −35.2 | 0.046 |
| **Dominant Model** | | | | | | | |
| rs1944577 | 18 | 45730103 | C/T | 0.29 | ZBTB7C | −55.2 | 0.006 |
| rs8043555 | 16 | 27777831 | G/A | 0.14 | KIAA0556 | 49.1 | 0.020 |
| rs11639671 | 16 | 27839368 | T/C | 0.36 | GSG1L | 41.6 | 0.040 |
| rs11074858 | 16 | 27429237 | C/T | 0.23 | IL21R | −40.1 | 0.042 |
| rs1489169 | 18 | 45875660 | G/A | 0.41 | ZBTB7C | −44.8 | 0.046 |
| **Recessive Model** | | | | | | | |
| rs1283687 | 8 | 108416439 | A/G | 0.23 | ANGPT1 | 187.1 | $3.94\times10^{-4}$ |
| rs10163610 | 18 | 45932358 | A/G | 0.14 | ZBTB7C | 146.6 | 0.008 |
| rs2514830 | 8 | 109015798 | C/A | 0.39 | RSPO2 | 60.1 | 0.021 |
| rs3091235 | 16 | 27442852 | G/A | 0.26 | IL21R | 89.8 | 0.026 |
| rs2189521 | 16 | 27413816 | T/C | 0.45 | IL21R | 52.5 | 0.032 |
| rs12934152 | 16 | 27414589 | T/C | 0.33 | IL21R | 71.9 | 0.036 |
| rs1000031 | 18 | 46361691 | G/A | 0.32 | CTIF | 60.3 | 0.046 |

*MAF is the minor allele frequency

†Beta is the correlation coefficient between SNP and infarct ratio based on the minor allele